

Simulating the response to phosphate additions in the oligotrophic eastern Mediterranean using an idealized four-member microbial food web model

T. Frede Thingstad

Department of Biology, Marine Microbiology Group, University of Bergen, PO Box 7800, N5020 Bergen, Norway

Received 18 June 2004; accepted 28 August 2005

Abstract

Elsewhere in this volume, observations of the natural microbial food web in the Cyprus Gyre, eastern Mediterranean, and its transient responses both to phosphate additions in situ and to phosphate and ammonium additions when enclosed in microcosm bottles, are reported. We here explore an idealized four-population model of the microbial part of the food web, containing features suggested in these reports to be essential for the observed responses. Such features include a steady state with P-limited growth heterotrophic bacteria and P-limited or N/P co-limited growth of phytoplankton a mechanism for luxury consumption and nutrient storage in the osmotrophs (phytoplankton and bacteria), a supply of labile organic carbon substrates in excess of bacterial carbon demand, a relatively small excess of bio-available nitrogen, and an assumption that heterotrophic bacteria are superior to phytoplankton in competing for dissolved organic nitrogen. From a P-limited steady-state dominated by heterotrophic organisms, the model responds to the in situ phosphate addition of the Lagrangian experiment with a decrease in chlorophyll, an increase in bacterial production and in bacterial biomass, and a decrease in uptake potential for phosphate. These modeled responses at the osmotroph level are qualitatively and quantitatively comparable to those observed, while detailed comparison of model and observations at the predator level appears more difficult. The model is also able to explain main traits of the dynamic patterns observed in microcosm experiments, both when different concentrations of phosphate were added to previously unperturbed water, and when water collected inside the patch of the Lagrangian experiment was enclosed and supplied with ammonia. We conclude that the idealized model contains sufficient elements to capture a useful first-order approximation to a presumably quite complex microbial food web. In this model, predator growth responds not only to food quantity, but also to food quality (stoichiometry). From steady states where also zooplankton are P-limited, the model thus has a potential for much more rapid zooplankton response to a phosphate-pulse than possible in models with fixed organism stoichiometry. The potential of transmitting a signal to the copepod level via food composition, rather than only via food abundance, is discussed. Implicit in both model and observations is a requirement of a large, unmeasured, production of degradable organic substrates for bacterial growth.

© 2005 Elsevier Ltd. All rights reserved.

Keywords: Food web models; Phosphate limitation; Lagrangian experiments; Mediterranean

E-mail address: frede.thingstad@bio.uib.no.

1. Introduction

The mixed surface layer of the Cyprus Gyre in the eastern Mediterranean is a typical low-nutrient-low-chlorophyll (LNLC) area with chlorophyll levels $<20 \mu\text{g m}^{-3}$ and free mineral forms of both phosphorous and nitrogen at very low concentrations in the stable summer situation (Krom et al., 1993). High nitrate:phosphate-ratios (Krom et al., 1991) and bioassay experiments for phytoplankton (Bonin et al., 1989) and heterotrophic bacteria (Zohary and Robarts, 1998) have suggested growth of these osmotrophs to be P-limited.

In a situation with one limiting mineral nutrient and all other potentially limiting nutrients in large excess, the conceptual model one would use to predict the system's response to an addition of the limiting nutrient would seem relatively straightforward. For example, prediction of a large phytoplankton bloom in response to iron addition to a high-nutrient-low-chlorophyll (HNLC) area (Coale et al., 1996) is consistent with the idea of iron-limitation. In the typical LNLC situation, however, neither the magnitude of the excess reservoirs of other non-limiting nutrients, nor the relative abilities of the different functional groups of micro-organisms to utilize these reservoirs are known. From present knowledge of such systems, it is thus far from easy to predict whether the response to an addition of the limiting nutrient will be substantial growth, will be restricted to a change in the physiological status of the organisms as the type of limitation suddenly is changed, or will cause a rebalance between organisms in the pelagic food web due to a sudden change in the requirement for competition abilities.

The response of a LNLC system to a Lagrangian nutrient perturbation is likely to be a relatively complex function of properties at scales ranging from the cell physiology of uptake, incorporation and storage of limiting and near-limiting nutrients, via trophic interactions such as predator responses to food quantity and quality, to the physical mixing with out-of-patch water, forcing a drift back towards the pre-perturbation state of the system. Although elements of such a response can be discussed in isolation, it rapidly becomes difficult to envisage how the different mechanisms work in concert.

As a tool to explore these relationships, and to confirm consistency between mechanisms proposed and responses observed, we here explore an

idealized four-population mathematical model of the microbial food web and compare it to observations reported elsewhere in this volume. The model is closely related to models previously used to analyze system responses in mesocosm experiments (Thingstad et al., 1999a, b), but includes the use of Droop formulations for heterotrophic bacteria and phytoplankton, shown in experimental laboratory systems to be required when details of shifts between situations with different limiting factors are studied (Thingstad and Pengerud, 1985; Pengerud et al., 1987; Thingstad, 1987). Combining potential N and P limitation with Droop formulations, the model has several traits resembling the more elaborate ERSEM model (Baretta-Bekker et al., 1997).

2. Models

In this oligotrophic system with a considerable fraction of phytoplankton biomass in small cyanobacteria (Psarra et al., 2005), we suspect heterotrophic flagellates to feed, not only on heterotrophic, but also on the autotrophic bacteria (Dolan, 1999; Christaki et al., 2001; Guillou et al., 2001; Christaki et al., 2002). The simple models used for more eutrophic environments assuming one predator with strict selectivity for each functional group of osmotrophs (Thingstad et al., 1999a, b) has therefore here been modified with the assumption that heterotrophic flagellates feed, with different selectivity, on both phytoplankton and bacteria. The resulting idealized food web structure with bacteria, phytoplankton, heterotrophic flagellates and ciliates is shown in Fig. 1. Assuming both phytoplankton and heterotrophic bacteria to be P-limited; food uptake to be proportional to food

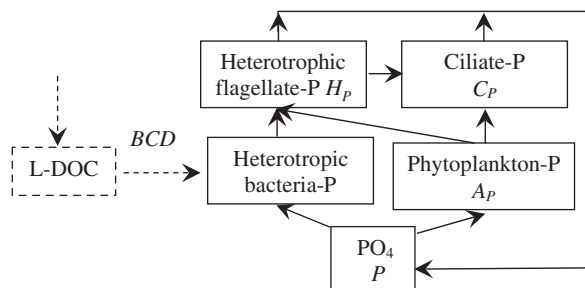


Fig. 1. Idealized food web used for analysis of steady state P-flow. Equations in Box 1. Labile dissolved organic carbon (L-DOC) is assumed to be in excess of bacterial carbon demand (BCD) and does therefore not enter the equations.

concentration; prey concentrations to be so low that predation on each type of prey is independent; a fixed loss rate for ciliates; and that all P released is

instantaneously remineralized to phosphate, the steady state distribution of P in the food web can be calculated (Box 1, Fig. 2).

Box 1

Simplified model (Fig. 1) used to calculate an analytical approximation to the steady state of the more complex simulation model of Fig. 2. Superscript * denotes analytical steady-state values for the simplified model in Fig. 1.

Assuming the system to be in steady state, the condition that **growth = loss** gives:
 for phytoplankton $\alpha'_{AP} P A_P = \beta_H \alpha'_H A_P H_P + \beta_C \alpha'_C A_P C_P$,

for heterotrophic bacteria $\alpha'_{BP} P B_P = \alpha'_H B_P H_P$,

for heterotrophic flagellates $Y_H \alpha'_H (B_P + \beta_H A_P) H_P = \alpha'_C H_P C_P$,

and for ciliates $Y_C \alpha'_C (H_P + \beta_C A_P) C_P = \delta_C C_P$.

Mass balance gives: $P_T = P + B_P + A_P + H_P + C_P$

Solving this set for the five state variables P , B_P , A_P , and H_P in terms of total-P P_T gives:

$$P^* = \frac{(P_T - ((1 - \beta_H)/Y_C \beta_C \alpha'_C) \delta_C)}{1 + (1 - (1/\beta_C)(1 - \beta_H((1 - (1/Y_H)) + (\alpha'_H/\alpha'_C))))(\alpha'_B/\alpha'_H) + ((1/Y_H \beta_C) + (\alpha'_H/\alpha'_C))\alpha'_A/\alpha'_H}$$

$$H_P^* = \frac{\alpha'_B}{\alpha'_H} P^*; \quad C_P^* = \frac{\alpha'_A - \beta_H \alpha'_B}{\beta_C \alpha'_C} P^*;$$

$$A_P^* = \frac{1}{\rho_C} \left(\frac{\delta_C}{Y_C \alpha'_C} - \frac{\alpha'_B}{\alpha'_H} P^* \right); \quad B_P^* = \left(\frac{\alpha'_C}{Y_H \alpha'_H} \frac{\alpha'_A - \beta_H \alpha'_B}{\beta_C \alpha'_C} + \frac{\beta_H \alpha'_B}{\beta_C \alpha'_H} \right) P^* - \frac{\beta_H}{\beta_C} \frac{\delta_C}{Y_C \alpha'_C}$$

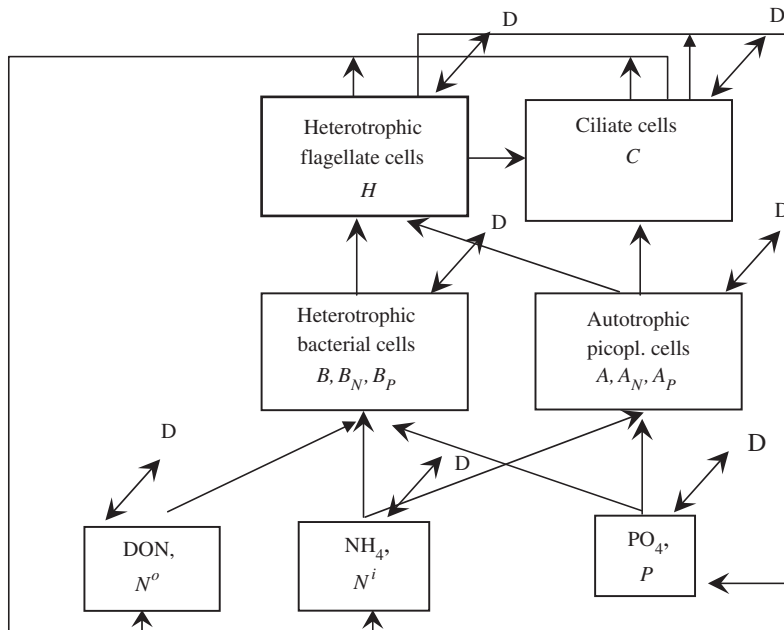


Fig. 2. Structure of simulation model used for comparison with observations. Grey arrows marked D denote physical dilution due to mixing with non-perturbed water masses.

As can be seen from the analytical solutions in **Box 1**, the steady-state values P^* , B_P^* , A_P^* , H_P^* , and C_P^* (see **Table 1** for symbols) depend not only on the parameters characterizing the organisms (affinity constants and clearance rates (α -parameters), yields (Y -parameters) and predation selectivities (β -parameters)), but also on P_T and δ_C representing total amount of bio-available phosphorous (sum of all compartments), and ciliate loss rate, respectively. δ_C is thus the parameterization of all predation pressure from higher predators.

Discussion of the properties of the steady state solution in **Box 1** is not a central issue of this article, but it is worth noticing that it contains some counter-intuitive aspects. One is that steady-state phytoplankton biomass A_P may appear to decrease, and finally become 0, as nutrient content P_T increases. This partly reflects the lack of other functional groups, such as e.g. diatoms avoiding ciliate predation in this model. It also reflects the lack of higher predators, the inclusion of which would imply that ciliate loss rate δ_C no longer could be considered a constant, independent of P_T . For a step-up perturbation in P_T , the model in **Fig. 1** can thus only aspire to reflect the behavior within the time-span before there is an appreciable numerical response in either higher predators such as copepods, or in the tiny diatom seed population present in this oligotrophic environment. The model would thus also not be expected to be able to catch the behavior of more eutrophic systems where a diatom-copepod link needs to be added to the food web to get the dynamics of the phytoplankton response to nutrient additions correct. With no explicit formulations of a C-budget, bacteria assumed always to have an excess of C-substrates, the model obviously does not aspire to reflect situations where bacterial growth becomes C-limited.

Although the working hypothesis here is that the simple P-flow model in **Fig. 1** is a useful first-order approximation to the steady state in the system under investigation, it is clearly insufficient for an analysis of experiments where phytoplankton and/or heterotrophic bacteria are driven into situations with growth limiting nutrients other than phosphate. Extending the model to include potential N-limitation could be done relatively simply by assuming fixed N:P-stoichiometry in all organisms. The only extra state variables required would then be those representing nonbiological forms of N such as ammonia and dissolved organic-N (DON). Such

a straight-forward extension seems, however, unable to explain some of the data we wanted the model to be able to simulate. A fixed-stoichiometry model would not be able to predict an increase in (living) particulate-P without a parallel increase in cell abundance; neither would it be able to predict a decrease in maximum potential for phosphate uptake without a parallel decrease in abundance of phosphate consuming organisms. The model chosen (**Box 2**, adapted from Thingstad, 1987) is therefore cell-based with variable cell quotas of N and P in heterotrophic bacteria and in phytoplankton. Cell-specific uptake (u) is assumed to follow a Michaelis–Menten relationship with external concentration, but the maximum uptake rate (v) is made a linear function of the internal cell quota of the limiting element (**Box 3**), reducing the uptake potential of the cell when the internal storage capacity for the given element is filled.

DON production is assumed to be a fixed fraction f_{DON} of the N released by heterotrophic flagellates and ciliates. The model also assumes that only heterotrophic bacteria can consume DON. While this may seem in accordance with what is usually believed for e.g. the uptake at low concentrations of amino-acids, this may be a simplification in the present case where the small prokaryotic members of the phytoplankton community may seem to have the potential to consume DON (Zubkov et al., 2003). Direct conversion of ammonia to DON as observed in e.g. *Synechococcus* (Bronk, 1999) is a process not included in this model.

Predation at low prey densities is weighted with selectivity parameters for phytoplankton (β_H , β_C) allowing different clearance rates for the types of prey available to each of the two groups of predators. At high prey densities predation is weighted with the carbon content of prey cells relative to that of the predator, assuming this to represent the handling time required for each type of prey. Cell quotas of carbon are assumed fixed in the protozoa, while fixed C:N-ratios are assumed for bacteria and phytoplankton. Ingestion is independent of prey stoichiometry in this model. The resulting growth of the predator, however, is calculated as the minimum of ingested phosphate, nitrogen, or carbon corrected for predator respiration, relative to predator cell quotas of the respective element. Predator growth rates can thus be C, N or P limited.

The diffusive mixing process of the Lagrangian experiment is represented here by a simple first

Table 1
List of symbols

Symbol	Meaning	Initial value/parameter value	Unit
<i>State variables</i>			
B	Bacterial abundance	8.15×10^7	cells l ⁻¹
A	Phytoplankton abundance	2.39×10^5	cells l ⁻¹
H	Heterotrophic flagellates	$H_P^0 Q_{HP}^{-1}$	cells l ⁻¹
C	Ciliate abundance	$C_P^0 Q_{CP}^{-1}$	cells l ⁻¹
B_P	P in biomass of heterotrophic bacteria	1.15	nM-P
A_P	P in biomass of phytoplankton	0.04	nM-P
(H_P)	P in biomass of heterotrophic flagellates	2.69	nM-P
(C_P)	P in biomass of ciliates	3.95	nM-P
P	Free orthophosphate	0.18	nM-P
B_N	N in biomass of heterotrophic bacteria	45.89	nM-N
A_N	N in biomass of phytoplankton	1.04	nM-N
(H_N)	N in biomass of heterotrophic flagellates	$H Q_{HN}$	nM-N
(C_N)	N in biomass of ciliates	$C Q_{CN}$	nM-N
N^i	Ammonia-N	5.30	nM-N
N^o	DON-N	41.11	nM-N
<i>Cell quotas and yields</i>			
Q_{BP}	Bacterial cell quota of P $Q_{BP} = B_P/B$	Function	nmol-P cell ⁻¹
Q_{BP}^{\min}	Minimum bacterial cell quota of P	1.11×10^{-8}	nmol-P cell ⁻¹
Q_{BP}^{\max}	Maximum bacterial cell quota of P	$5 Q_{BP}^{\min}$	nmol-P cell ⁻¹
Q_{BN}	Bacterial cell quota of N $Q_{BN} = B_N/B$	Function	nmol-N cell ⁻¹
Q_{BN}^{\min}	Minimum bacterial cell quota of N	$25 Q_{BP}^{\min}$	nmol-N cell ⁻¹
Q_{BN}^{\max}	Maximum bacterial cell quota of N	$2.5 Q_{BN}^{\min}$	nmol-N cell ⁻¹
Q_{BC}	Bacterial cell quota of C	$5 Q_{BN}$	nmol-C cell ⁻¹
Q_{AP}	Phytoplankton cell quota of P $Q_{AP} = A_P/A$	Function	nmol-P cell ⁻¹
Q_{AP}^{\min}	Minimum phytoplankton cell quota of P	$10 Q_{BP}^{\min}$	nmol-P cell ⁻¹
Q_{AP}^{\max}	Maximum phytoplankton cell quota of P	$5 Q_{AP}^{\min}$	nmol-P cell ⁻¹
Q_{AN}	Phytoplankton cell quota of N $Q_{AN} = A_N/A$	Function	nmol-N cell ⁻¹
Q_{AN}^{\min}	Minimum phytoplankton cell quota of N	$25 Q_{AP}^{\min}$	nmol-N cell ⁻¹
Q_{AN}^{\max}	Maximum phytoplankton cell quota of N	$2.5 Q_{AN}^{\min}$	nmol-N cell ⁻¹
Q_{AC}	Phytoplankton cell quota of C	$(106/16) \cdot 8 Q_{AN}$	nmol-C cell ⁻¹
Q_{HP}	Het. flag. cell quota of P	$27 Q_{AP}^{\min}$	nmol-P cell ⁻¹
Q_{HN}	Het. flag. cell quota of N	$16 Q_{HP}$	nmol-N cell ⁻¹
Q_{HC}	Het. flag. cell quota of C	$106 Q_{HP}$	nmol-C cell ⁻¹
Q_{CP}	Ciliate cell quota of P	$1000 Q_{HP}$	nmol-P cell ⁻¹
Q_{CN}	Ciliate cell quota of N	$16 Q_{CP}$	nmol-N cell ⁻¹
Q_{CC}	Ciliate cell quota of C	$106 Q_{CP}$	nmol-C cell ⁻¹
r_H	Fraction of prey C respired by heterotrophic flagellates	0.5	—
r_C	Fraction of prey C respired by ciliates	0.5	—
Y_H	Fraction of prey-P incorporated by heterotrophic flagellates	Not used in simulation model	—
Y_C	Fraction of prey-P incorporated by ciliates	Not used in simulation model	—
<i>Rates</i>			
δ_C	Specific loss rate of ciliates	0.1/24	h ⁻¹
D	Dilution rate of patch	0.62/24	h ⁻¹
v_{XY}	Specific uptake rate of substrate Y by population X	Functions	nM-Y cell ⁻¹ h ⁻¹
Ω_{XY}	Predation rate by predator X on prey Y	Functions	prey cells l ⁻¹ h ⁻¹
I_H^{\max}	Maximum ingestion rate of H	5/24	Predator cell equivalents l ⁻¹ h ⁻¹
I_C^{\max}	Maximum ingestion rate of C	5/24	Predator cell equivalents l ⁻¹ h ⁻¹
<i>Cell-specific affinity constants, clearance rates and selectivity constants</i>			
Primed affinity constants represent biomass-P-specific constants so that $\alpha'_{XY} = \alpha_{XY}/Q_{XY}$			
α_{BP}	Bacterial cell-specific affinity for phosphate*	$0.16 Q_{BP}^{\min}$	l cell ⁻¹ h ⁻¹

Table 1 (continued)

Symbol	Meaning	Initial value/parameter value	Unit
α_{BN^i}	Bacterial cell-specific affinity for ammonia	α_{BP}	$1 \text{ cell}^{-1} \text{ h}^{-1}$
α_{BN^o}	Bacterial cell-specific affinity for DON	$0.1 \alpha_{BN^i}$	$1 \text{ cell}^{-1} \text{ h}^{-1}$
α_{AP}	Phytoplankton cell-specific affinity for phosphate	$0.18 Q_{AP}^{\min}$	$1 \text{ cell}^{-1} \text{ h}^{-1}$
α_{AN^i}	Phytoplankton cell-specific affinity for ammonia	α_{AP}	$1 \text{ cell}^{-1} \text{ h}^{-1}$
α_{HB}	Heterotrophic flagellate cell-specific clearance rate for heterotrophic bacteria	$0.009 Q_{HP}$	$1 \text{ cell}^{-1} \text{ h}^{-1}$
α_{CH}	Ciliate clearance rate for heterotrophic flagellates	$0.0025 Q_{CP}$	$1 \text{ cell}^{-1} \text{ h}^{-1}$
β_H	Heterotrophic flagellate selectivity of <i>A</i> relative to <i>B</i>	0.3	—
β_C	Ciliate selectivity of <i>A</i> relative to <i>H</i>	1.5	—
u_{XY}	Cell-specific uptake rate of substrate <i>Y</i> (P, N ⁱ or N ^o) by population <i>X</i> (<i>A</i> or <i>B</i>)	Function	$\text{nmol-Y cell}^{-1} \text{ h}^{-1}$
v_{XY}	Maximum cell specific uptake rate by population <i>X</i> at high external concentration of substrate <i>Y</i> for a given cell quota of <i>Y</i>	Functions	$\text{nmol-Y cell}^{-1} \text{ h}^{-1}$
v_{BP}^{\max}	Maximum obtainable cell-specific uptake rate for P by B	$(Q_{BP}^{\max} - Q_{BP}^{\min})/2.5$	$\text{nmol-P cell}^{-1} \text{ h}^{-1}$
$v_{BN^i}^{\max}$	Maximum specific uptake rate for ammonia by B	$(Q_{BN}^{\max} - Q_{BN}^{\min})/4$	$\text{nmol-N cell}^{-1} \text{ h}^{-1}$
$v_{BN^o}^{\max}$	Maximum specific uptake rate for DON by B	$0.5 v_{BN^i}^{\max}$	$\text{nmol-N cell}^{-1} \text{ h}^{-1}$
v_{AP}^{\max}	Maximum. specific uptake rate for phosphate by A	$(Q_{AP}^{\max} - Q_{AP}^{\min})/2.5$	$\text{nmol-P cell}^{-1} \text{ h}^{-1}$
v_{AN}^{\max}	Maximum. specific uptake rate for ammonia by A	$(Q_{AN}^{\max} - Q_{AN}^{\min})/4$	$\text{nmol-P cell}^{-1} \text{ h}^{-1}$
<i>Miscellaneous</i>			
f_{DON}	Fraction of N released from biota as DON Chlorophyll per phytoplankton cell*	0.4 $Q_{AC} A \times \frac{12}{35}$	— ng Chla cell^{-1}

Symbols in parentheses are not independent state variables but follow from the assumption of fixed per cell contents.

order “chemostat type” dilution where the community in the dilution water is the steady-state community. This steady-state community was obtained in a two-step process by initiating a simulation run of the dynamic model with the analytically solved steady state for the simplified model (Box 1), running the dynamic model to its steady state, and then setting the initial values equal to values in the dilution water equal to the steady state obtained by letting the model run to steady state.

The simulations were performed on a WindowsTM-based PC using the Berkeley MadonnaTM software with its auto step-size routine for solving the differential equations.

3. Comments to parameter values listed in Table 1

The minimum cell quota of P in bacteria $Q_{BP}^{\min} = 1.11 \times 10^{-8} \text{ nmol-P cell}^{-1}$ would, with a standard

50:1 molar C:P-ratio in bacterial biomass (Fagerbakke et al., 1996) correspond to ca 7 fg-C cell⁻¹ i.e. a cell slightly less than half the C-biomass of a “standard” 20 fg-C cell⁻¹ bacterium (Lee and Fuhrman, 1987). Phytoplankton cells have a minimum cell quota of P $Q_{AP}^{\min} = 10 Q_{BP}^{\min}$, corresponding to an assumption of the linear dimension of phytoplankton be about 3 times larger than for heterotrophic bacteria, i.e. corresponding to small pico-planktonic forms of phytoplankton.

The phytoplankton and bacteria cell-specific affinity constants $\alpha_{AP} = 0.18 Q_{AP}^{\min}$ and $\alpha_{BP} = 0.16 Q_{BP}^{\min} 1 \text{ cell}^{-1} \text{ h}^{-1}$ are consistent with the biomass-P specific value $\alpha'_{AP} = 0.16 - 0.20 1 \text{ nmol-P}^{-1} \text{ h}^{-1}$, determined experimentally in the eastern Mediterranean by Moutin et al. (2002).

Both groups of osmotrophs are assumed to have a maximum cell quota of P five times the minimum quota, i.e. enough for >2 cell doublings. The

Box 2

Differential equations of the simulation model.

Bacterial cell abundance:	$\frac{dB}{dt} = \mu_B B - \Omega_{HB} + D(B^0 - B)$
Phytoplankton abundance:	$\frac{dA}{dt} = \mu_A A - \Omega_{HA} - S_{CA} + D(A^0 - A)$
Heterotrophic flagellate abundance:	$\frac{dH}{dt} = G_H - \Omega_{CH} + D(H^0 - H)$
Ciliate abundance:	$\frac{dC}{dt} = G_C - \delta_C C + D(C^0 - C)$
Bacterial-P:	$\frac{dB_P}{dt} = v_{BP} B - Q_{BP} \Omega_{HB} + D(B_P^0 - B_P)$
Bacterial-N:	$\frac{dB_{N^i}}{dt} = (v_{BN^i} + v_{BN^o}) B - Q_{BN} \Omega_{HB} + D(B_{N^i}^0 - B_{N^i})$
Phytoplankton-P:	$\frac{dA_P}{dt} = v_{AP} A - Q_{AP} (\Omega_{HA} + \Omega_{CA}) + D(A_P^0 - A_P)$
Phytoplankton-N:	$\frac{dA_{N^i}}{dt} = v_{AN^i} A - Q_{AN} (\Omega_{HA} + \Omega_{CA}) + D(A_{N^i}^0 - A_{N^i})$
Phosphate:	$\frac{dP}{dt} = (\Omega_{HA} Q_{AP} + \Omega_{HB} Q_{BP} - G_H Q_{HP}) + (\Omega_{CA} Q_{AP} + \Omega_{CH} Q_{HP} - G_C Q_{CP})$ $+ \delta_C Q_{CP} C - u_{BP} B - u_{AP} A + D(P^0 - P)$
Ammonia:	$\frac{dN^i}{dt} = (1 - f_{DON}) ((\Omega_{HA} Q_{AN} + \Omega_{HB} Q_{BN} - G_H Q_{HN}) + (\Omega_{CA} Q_{AN} + \Omega_{CH} Q_{HN} - G_C Q_{CN}) + \delta_C C Q_{CN})$ $- u_{AN^i} A - u_{BN^i} B + D(N^{i0} - N^i)$
DON:	$\frac{dN^o}{dt} = f_{DON} ((\Omega_{HA} Q_{AN} + \Omega_{HB} Q_{BN} - G_H Q_{HN})$ $+ (\Omega_{CA} Q_{AN} + \Omega_{CH} Q_{HN} - G_C Q_{CN}) + \delta_C C Q_{CN})$ $- u_{BN^o} B + D(N^{o0} - N^o)$

maximum cell specific uptake rates (v^{\max}) are given values which, if uptake was kept running constant at this rate, could fill the cells from minimum to maximum cell quota in 2.5 h. Heterotrophic flagellate cells are assumed to have a cell quota of P $Q_{HP} = 27 Q_{AP}^{\min}$, i.e. corresponding to a factor 3 in linear size between the heterotrophic flagellates and the phytoplankton (assumed to be dominantly autotrophic picoplankton). Ciliates are assumed 10 times larger in linear size than heterotrophic flagellates. Both heterotrophic flagellates and ciliates are assumed to be able, at infinite food concentrations, to ingest five times their own cell quota of carbon per day.

Cell-specific affinity constants for ammonium are set equal to the corresponding values for phosphate $\alpha_{XN}^i = \alpha_{XP}$; $X = A$ or B , assuming the main determinant for these to be the diffusion rate of

small molecules in seawater. Bacterial cell-specific affinity for DON is set to half that of ammonia $\alpha_{BN^o} = 0.1 \alpha_{BN^i}$, assuming the diffusion of these larger molecules to be considerably slower than that of small molecules. This also includes an implicit parameterization of the hydrolysis step from proteins to amino-acids. Also the maximum uptake rate for DON is set to half that for ammonia $v_{BN^o}^{\max} = 0.5 v_{BN^i}^{\max}$. The fraction f_{DON} of N-release from the biota that is in the form of DON is set to 0.4, the rest $(1 - f_{DON})$ is released as ammonia. An important consequence of these choices is a distribution of dissolved N in the P-limited steady state with most of the excess-N in the DON-pool, and thus a larger pool of N available to heterotrophic bacteria than to phytoplankton when the system is perturbed with addition of phosphate. Interestingly, a more extreme choices of these parameters can give a steady

Box 3

Representation of biological rates in the simulation model.

Cell-quota dependent maximum cell specific uptake rate of phosphate, ammonia and DON:

Bacteria:

$$v_{BP} = v_{BP}^{\max} \frac{Q_{BP}^{\max} - Q_{BP}}{Q_{BP}^{\max} - Q_{BP}^{\min}}; \quad v_{BN^i} = v_{BN^i}^{\max} \frac{Q_{BN}^{\max} - Q_{BN}}{Q_{BN}^{\max} - Q_{BN}^{\min}}; \quad v_{BN^o} = v_{BN^o}^{\max} \frac{Q_{BN}^{\max} - Q_{BN}}{Q_{BN}^{\max} - Q_{BN}^{\min}}$$

Phytoplankton:

$$v_{AP} = v_{AP}^{\max} \frac{Q_{AP}^{\max} - Q_{AP}}{Q_{AP}^{\max} - Q_{AP}^{\min}};$$

$$v_{BN^i} = v_{BN^i}^{\max} \frac{Q_{AN}^{\max} - Q_{AN}}{Q_{AN}^{\max} - Q_{AN}^{\min}}; \quad (\text{no phytoplankton uptake of DON})$$

Per cell specific rate of phosphate, ammonia, and DON uptake:

Bacteria:

$$u_{BP} = \frac{\alpha_{BP}P}{1 + (\alpha_{BP}/v_{BP})P}; \quad u_{BN^i} = \frac{\alpha_{BN^i}N^i}{1 + (\alpha_{BN^i}/v_{BN^i})N^i}; \quad u_{BN^o} = \frac{\alpha_{BN^o}N^o}{1 + (\alpha_{BN^o}/v_{BN^o})N^o}$$

Phytoplankton:

$$u_{AP} = \frac{\alpha_{AP}P}{1 + (\alpha_{AP}/v_{AP})P}; \quad u_{BN^i} = \frac{\alpha_{AN^i}N^i}{1 + (\alpha_{AN^i}N^i/v_{AN})}$$

Specific growth rates:

Bacteria:

$$\mu_B = \mu_B^{\max} \left(1 - \max \left(\frac{Q_{BP}^{\min}}{Q_{BP}}, \frac{Q_{BN}^{\min}}{Q_{BN}} \right) \right);$$

$$\text{phytoplankton} : \mu_A = \mu_A^{\max} \left(1 - \max \left(\frac{Q_{AP}^{\min}}{Q_{AP}}, \frac{Q_{AN}^{\min}}{Q_{AN}} \right) \right)$$

Predation rates (prey cells consumed $l^{-1} h^{-1}$):

$$\text{H on B} : \Omega_{HB} = \frac{\alpha_{HB}B}{1 + (\alpha_{HB}(B(Q_{BC}/Q_{HC}) + \beta_{HA}A(Q_{AC}/Q_{HC}))/I_H^{\max}(Q_{BC}/Q_{HC}))};$$

$$\text{H on A} : \Omega_{HA} = \frac{\alpha_{HB}\beta_{HA}A}{1 + \alpha_{HB}(B(Q_{BC}/Q_{HC}) + \beta_{HA}A(Q_{AC}/Q_{HC}))/I_H^{\max}(Q_{AC}/Q_{HC})}$$

$$\text{C on H} : \Omega_{CH} = \frac{\alpha_{CH}H}{1 + \alpha_{CH}(H(Q_{HC}/Q_{CC}) + \beta_{CA}A(Q_{AC}/Q_{CC}))/I_C^{\max}(Q_{HC}/Q_{CC})};$$

$$\text{C on A} : \Omega_{CA} = \frac{\alpha_{CH}\beta_{CA}A}{1 + \alpha_{CH}(H(Q_{HC}/Q_{CC}) + \beta_{CA}A(Q_{AC}/Q_{CC}))/I_C^{\max}(Q_{AC}/Q_{CC})}$$

Growth of heterotrophic flagellates:

$$G_H = \min \left(\frac{\Omega_{HB}Q_{BP} + \Omega_{HA}Q_{AP}}{Q_{HP}}; \frac{\Omega_{HB}Q_{BN} + \Omega_{HA}Q_{AN}}{Q_{HN}}; \left(\frac{\Omega_{HB}Q_{BC} + \Omega_{HA}Q_{AC}}{Q_{HC}} \right) (1 - r_H) \right)$$

Growth of ciliates:

$$G_C = \min \left(\frac{\Omega_{CA}Q_{AP} + \Omega_{CH}Q_{HP}}{Q_{CP}}; \frac{\Omega_{CA}Q_{AN} + \Omega_{CH}Q_{HN}}{Q_{CN}}; \left(\frac{\Omega_{CA}Q_{AC} + \Omega_{CH}Q_{HC}}{Q_{CC}} \right) (1 - r_C) \right)$$

state (not shown) with P-limited heterotrophic bacteria and excess-N stored mainly in the DON-pool, but with N-limited phytoplankton unable to access the N stored in the DON pool. The system was started in a steady state with 8.0 nM total-P and 200 nM total-N, corresponding to a total N:P ratio of 25 and an excess-N of 72 nM-N relative to a system balanced at the Redfield ratio of 16.

Chlorophyll is converted from phytoplankton biomass-C with a fixed carbon:chlorophyll-ratio (w:w) of 35.

4. Simulation results

4.1. Microcosm experiments

We have challenged the model with two microcosm experiments, one is the 2001 experiment where surface water was incubated on-deck in 81 containers with a range of different orthophosphate concentrations added (Flaten et al., 2005). The other is the 2002 experiment where surface water was collected inside and outside the patch 3 days after the in situ addition, and then incubated with and without the addition of ammonium (Zohary et al., 2005). A sensitive indicator of the system's response dynamics to phosphate addition is the turnover-time T_t for orthophosphate. Adding phosphate to a

P-limited system with all other nutrients in excess of the added dose, one would expect an oscillatory pattern for T_t : from low values in the initial P-limited state to high values immediately afterwards when phosphate concentration is high. Then a decrease to low values as the added P is transformed to a high biomass of phytoplankton and/or heterotrophic bacteria competing for a now depleted orthophosphate reservoir, then a return to longer turnover-times as the P moves up the food chain to predators, producing a system with fewer phosphate competitors and more remineralization. If other limiting nutrients prevent consumption of the added phosphate, turnover-times will remain high.

The model is able to reproduce the pattern found experimentally in the 2001 microcosm experiment with an oscillating pattern for the 10 nM phosphate addition, but stable and high turnover-times when 25 nM or more was added (Fig. 3). The reasonable agreement between the period of the oscillation simulated and observed for the 10 nM addition suggest that the dynamics of phosphorous transfer through the model food chain occurs on realistic time scales.

For the experiment with addition of ammonia to water collected in- and out-side the experimental patch, the challenge to the model is more severe. Here the model is required to (1) calculate a steady

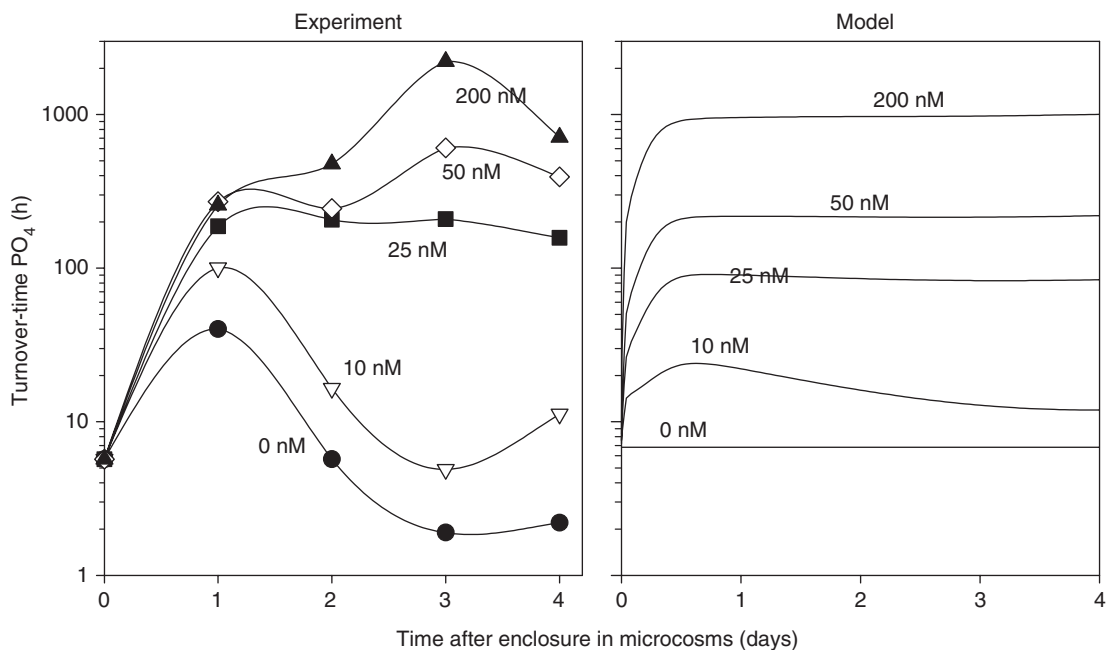


Fig. 3. Microcosm experiment 2001. Observed (left) and simulated (right) response in orthophosphate turnover-time T_t to different concentrations of orthophosphate added at time zero. Observations from Flaten et al. (2005).

state that fits the results observed in water collected outside the patch, (2) calculate the state inside the patch after 3 days, and (3) calculate the response when such water is enclosed with and without addition of ammonia. The model (Fig. 4) was able to correctly predict the turnover-time in the collected water, and ammonia to induce a bloom leading to a rapid reduction in orthophosphate turnover-time. The modeled dynamics of the bloom appears to be slightly too fast and a rapid succession of predators to the ammonia-induced bloom led to a modeled increase in turnover-time, not observed within the 4 day duration of the microcosm experiment (Fig. 4). The model response to the particular situation with both ammonia and phosphate added could be slowed down by decreasing the maximum specific growth rates μ_A^{\max} and μ_B^{\max} (not shown). The microcosm experiment was performed with water pre-filtered on a 200 μm mesh (Zohary et al., 2005) removing large zooplankton. We have not attempted to include this part of the manipulations in the simulations.

4.2. Lagrangian experiment

With the parameters used, the initial state had P-limited phytoplankton, heterotrophic bacteria,

and heterotrophic flagellates, while ciliates were C-limited (Fig. 5). The 110 nM phosphate addition shifted the modeled phytoplankton and bacteria to N-limitation, while the heterotrophic flagellates were shifted to C-limitation (Fig. 5). Heterotrophic bacteria, with their access to DON, returned to P-limitation 7.7 days after perturbation. With the conditions used, phytoplankton, with their access

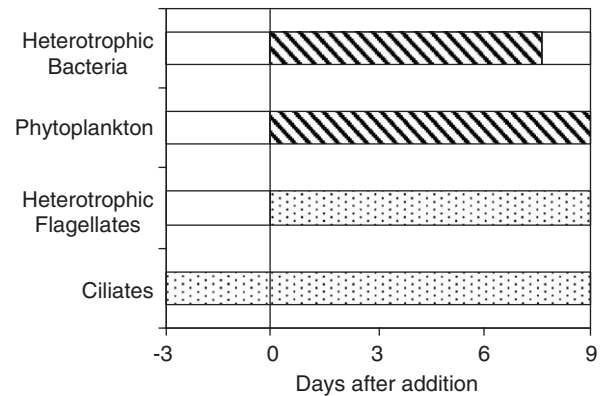


Fig. 5. Simulation of the Lagrangian experiment. Change in growth rate limiting element with time during simulation of Lagrangian experiment. Open bar: P-limitation, hatched bar: N-limitation, dotted bar: C-limitation.

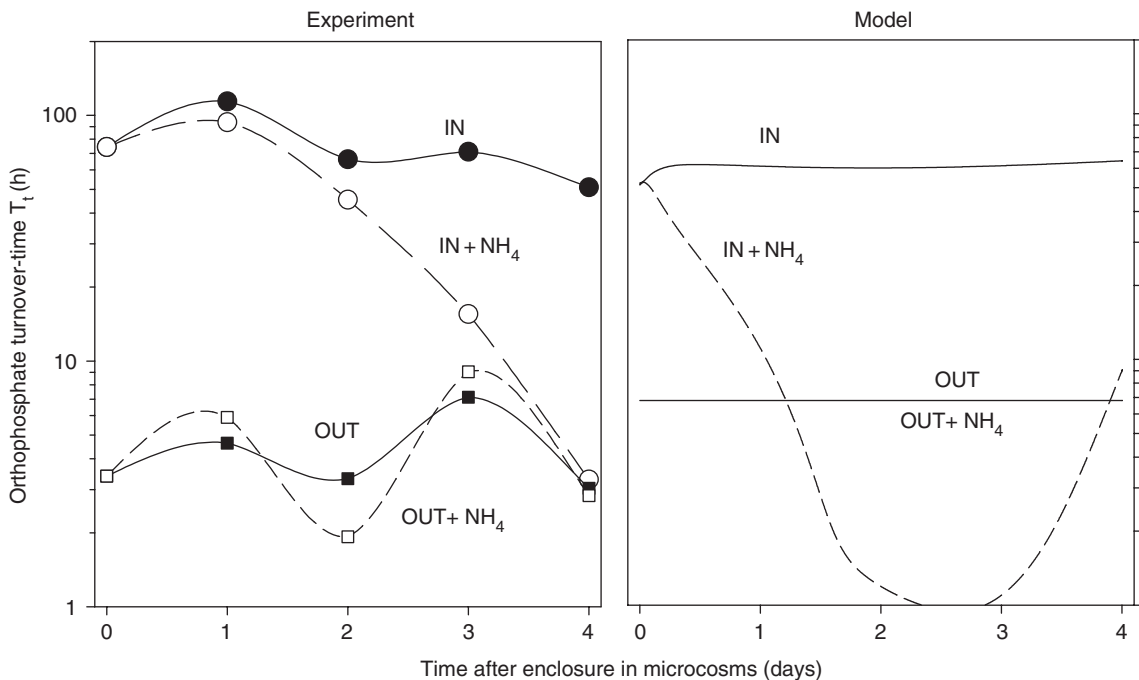


Fig. 4. Microcosm experiment 2002. Observed (left) and simulated (right) responses to on-deck incubation of water taken inside (circles) and outside (squares) the experimental patch 3 days after in situ addition of phosphate. Samples were incubated with (open symbols, broken lines) or without (filled symbols, solid lines) addition of 1600 nM ammonia at time = 0.

only to the ammonia pool, returned to P-limitation after 10.9 days (i.e. after the end of the observational period, not shown in Fig. 5).

The initial increase and subsequent decay back to background level observed for orthophosphate turnover-time was reasonably well reproduced by the model (Fig. 6A). A similar pattern was simulated for orthophosphate concentration (Fig. 6B), well in agreement with estimates of bioavailable orthophosphate obtained by isotope dilution bioassays (Flaten et al., 2005).

Due to saturation of the internal storage capacity for phosphorous in N-limited phytoplankton and bacteria, the model's maximum uptake potential for phosphate ($v_{AP} + v_{BP}$) dropped rapidly after the addition and remained low until the transition period back towards P-limitation, well in agreement with observations (Fig. 6C). Interestingly, the modeled peak in maximum uptake potential during the transition period between two limitations may seem to be reflected in the observations.

The model responded to phosphate addition with a slight decrease in primary production, a response not distinguishable from the observed (Fig. 7). For the decrease in chlorophyll there was also a good agreement between observations and model (Fig. 8A). Several aspects of the model seem to contribute to this somewhat counter-intuitive response in a P-limited system. This includes a higher maximum growth rate in heterotrophic bacteria than in phytoplankton ($\mu_B^{\max} > \mu_A^{\max}$), a greater access to N for heterotrophic bacteria than for phytoplankton (only bacteria have access to DON), and the assumption of an excess of labile DOC

available to the bacteria. The succession from growing heterotrophic bacteria to heterotrophic flagellates and ciliates, both assumed to prey on the phytoplankton thus induces a negative phytoplankton response in the model.

The modeled increase in bacterial production (Fig. 7B), and to some extent the increase in abundance (Fig. 8B), reflects the observations.

Particulate phosphorous was calculated for the model as the sum of cell abundances multiplied by their cell quotas. The initial model response in particulate-P is thus dominated by the change in bacterial and phytoplankton cell quotas as they shift to N-limitation. The model reasonably well reproduces the observed changes in particulate-P (Fig. 9).

The modelled biomass level for heterotrophic flagellates is in reasonable agreement with observations (Fig. 10), while the ciliate level is high with a factor of ca. 5. Interestingly, the size-spectra measured for particulate-P (Flaten et al., 2005) suggested greater biomass in the $>10\ \mu\text{m}$ fraction than could be calculated from the microscopic observations. The model predicts little microzooplankton responses to the phosphate addition. With a different initial state characterized by clear P-limitation of both heterotrophic flagellates and ciliates, a larger microzooplankton response would have been expected with this model.

5. Discussion

Much more interesting than how much biological detail can be incorporated into a mathematical model, is how much detail can be removed without

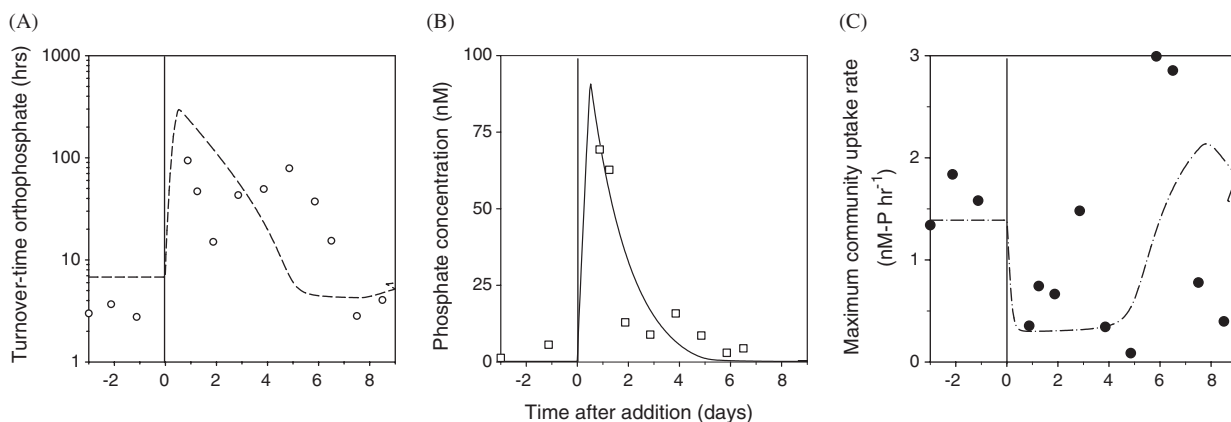


Fig. 6. Simulation of the Lagrangian experiment. (A) Orthophosphate turnover-time T_t modeled (broken line) and measured (open circles), (B) orthophosphate concentration modeled (solid line) and measured $K_1 + S_n$ (open squares) and maximum uptake rate for phosphate modeled (line-dot-line) and measured (solid circles). Observational data from Flaten et al. (2005).

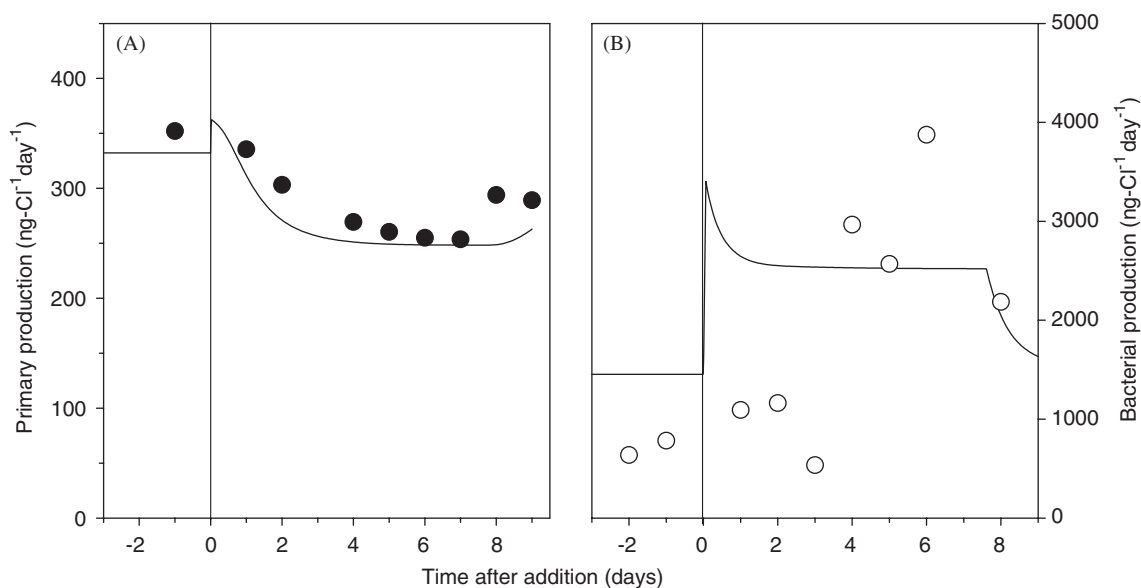


Fig. 7. Primary (A) and bacterial (B) production measured (circles) and simulated (lines). Experimental data for the Lagrangian experiment averaged for 0–16 m samples, observational data from Psarra et al. (2005) and Pitta et al. (2005).

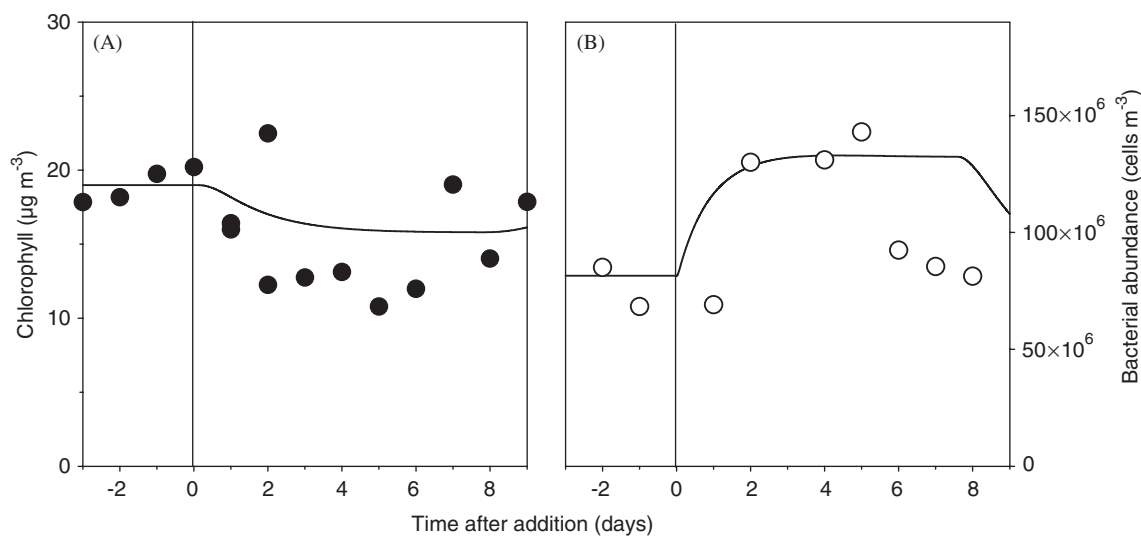


Fig. 8. Chlorophyll-*a* (A) and bacterial abundance (B). Observed (circles) and simulated (lines) values. Observed values from Pitta et al. (2005) averaged over 16 m.

removing the essential explanatory power of the model. From this perspective, the proposed model with its 11 state variables and > 35 parameters may appear uncomfortably complex. This complexity as measured in variables and parameters is the inevitable consequence of going from fixed stoichiometry to a Droop-type formulation of nutrient-

limited microbial growth. Without some kind of formulation with a feed-back from cell-quota to uptake potential, it is, however, difficult to see how responses such as e.g. the decrease in uptake potential (Fig. 6C) when limiting nutrient is added, could be simulated. For simulations of the system not requiring descriptions of shifts between P- and

N-limitation, simpler versions more similar to the version described in Fig. 1 and Box 1 would be preferable.

Seen from a biologist's point of view on the other hand, the model is not complex. Luxury consumption and flexible stoichiometry are well-described phenomena in both phytoplankton (e.g. Cochlan and Harrison, 1991; Jansson, 1993) and hetero-

trophic bacteria (Martinussen and Thingstad, 1987; Vadstein et al., 1988; Vadstein and Olsen, 1989; Vadstein, 1997), and the attempt here to reduce microbial diversity to four functional groups may appear extreme.

There are indeed interesting aspects of the system that would require further complexity if included in the model description. Studying the size-spectrum of phosphate uptake, the observed response in the Lagrangian experiment was a shift towards larger size-classes (Flaten et al., 2005). The model used here has a positive response for heterotrophic bacteria, and a negative for phytoplankton, and would thus presumably shift uptake towards smaller, rather than larger organisms. Additional mechanisms leading either to an increase in cell size during N-limitation, or to shift in phosphate consumption towards phytoplankton species belonging to larger size-classes, would seem required to simulate this observation.

Fitting the proposed model to a set of data with much higher bacterial production than particulate primary production implies that ciliates will get most of their food via heterotrophic flagellates. Since both ciliates and heterotrophic flagellates have a fixed Redfield stoichiometry of their biomass, there is a strong tendency for a steady state with

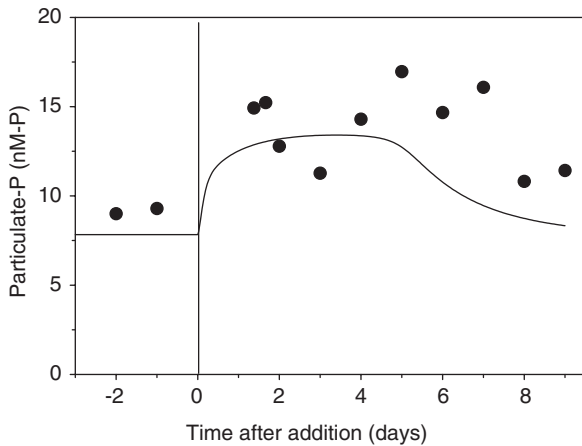


Fig. 9. Particulate-P measured (solid circles) and simulated (solid line). Observational data from Flaten et al. (2005) averaged for 0–16 m.

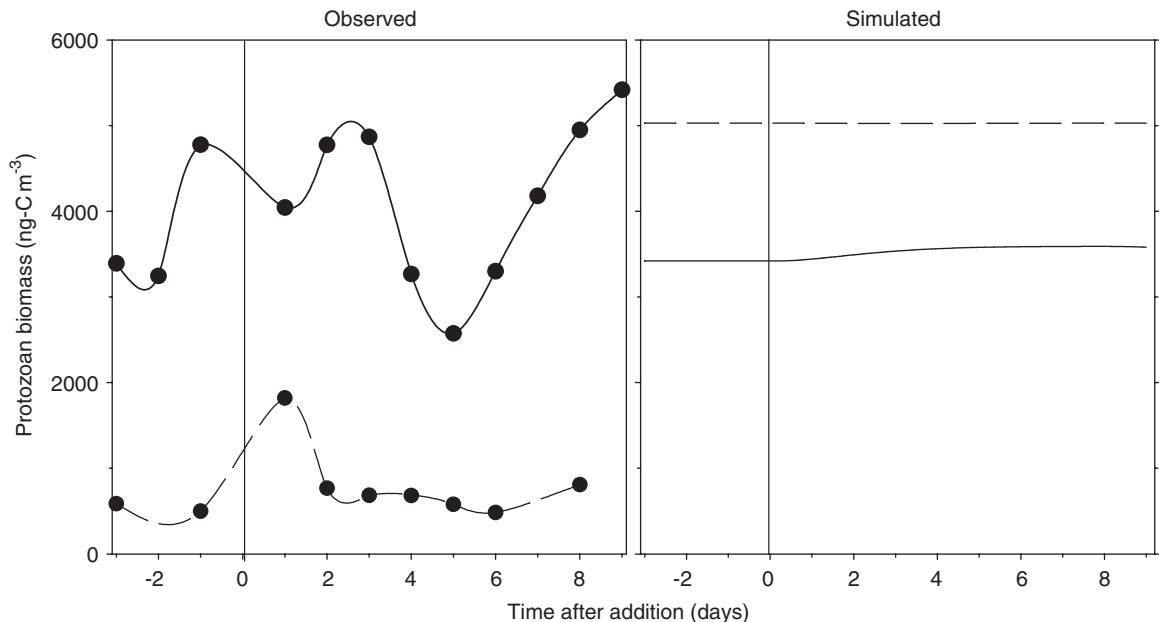


Fig. 10. Observed (A) and simulated (B) protozoan biomass during the Lagrangian experiment. Heterotrophic flagellates in the size class 2–10 μm (solid line, filled circles), and the model's heterotrophic flagellates (solid line), observed ciliates (open circles, broken line) and the model's ciliates (broken line). Observational data from Pitta et al. (2005), averaged from 0–16 m.

C-limited ciliates. Fitting the model to a higher primary production, more of the ciliate food will consist of P-depleted phytoplankton, and one can easily obtain steady states with P-limited ciliates (not shown). Since ciliate growth rate then responds to the rapid change in prey P-content, rather than to a change in prey abundance, ciliate response to a phosphate pulse becomes much faster than from the steady state used here. In the observations there were indications of rapid predator response to the added phosphate, both in ciliates (Psarra et al., 2005), and in copepod egg production (Pasternak et al., 2005). We therefore suspect that the C-limitation at predator level in our simulation may not be a correct representation of system. The system also contained a substantial fraction of mixotrophs (Pitta et al., 2005), blurring the strict distinction between osmotrophs and phagotrophs used in the model, thus further complicating a comparison between our model's idealized functional groups and observations.

The lack of functional groups of larger-sized phytoplankton has also prevented us from challenging this model with the microcosm experiment done in Haifa in year 2000 where there was a large response in diatoms (Kress et al., 2005). With diatoms to a large extent escaping the predation pressure from ciliates, we see no immediate reason not to expect the proposed model, expanded to include diatoms, to be able to explain a positive chlorophyll response in more nutrient-rich waters containing a significant diatom seed population. Adding diatoms to the present model would give a food web structure resembling the one proposed earlier as a generic framework for the microbial food web (Thingstad and Rassoulzadegan, 1995).

The model highlights some points that may be central to understanding how the eastern Mediterranean surface ecosystem functions. One is the possible “bypass” of added P around the phytoplankton community to their predators, thereby increasing phytoplankton loss rate (Thingstad et al. 2005). In our model, phytoplankton growth is limited due their inability to access the DON-pool with a negative change in net growth as the result. Shifting the model parameters so that the steady state has more of the excess-N in the DON pool and less in the ammonium pool, one can actually obtain a steady state with N-limited phytoplankton (not shown), despite the presence an excess of N in the system. Another potentially important aspect for the fate of nutrient pulses is the potential for

transfer of the P-pulse by a “trophic tunnelling” (Thingstad et al. 2005) where the added phosphate-P is rapidly taken up by luxury consumption in P-starved osmotrophs and P-starved predators then respond rapidly to this change in food quality. The responses at higher trophic level could with such a model be much faster than in a traditional fixed-stoichiometry model. In the eastern Mediterranean with its pulsed nutrient input from Saharan dust storms, such mechanisms could shorten the transfer time of the signal to copepods, and thus to fish production, considerably. If so, it seems that the discussion of whether P-limitation may possibly extend up the food chain to the zooplankton level, so far primarily an issue in the limnological literature (e.g. Andersen, 1997) may be of high relevance to the eastern Mediterranean.

With the assumption of a steady state with P-limited bacteria, the implicit requirement is that the system has a production, or an accumulated reservoir, of labile organic substrates sufficient to support the bacterial carbon demand. Turley et al. (2000) estimated a bacterial growth efficiency of 22% for the eastern Mediterranean. With this value, daily bacterial carbon demand would be $\sim 10 \mu\text{g-C l}^{-1}\text{day}^{-1}$. Theoretically, one might argue that excretion of newly photosynthesized organic material, not measured as ^{14}C on filters, may be likely to occur under severe P-starvation (e.g. Dubinsky and Berman-Frank, 2001), but to balance the C-budget in the present case, such DOC production would have to exceed the primary production of particulate-C ($\sim 0.35 \mu\text{g-C l}^{-1}\text{day}^{-1}$) by more than an order of magnitude. DOC concentration in the upper layer was ca. $100 \mu\text{M}$ (Krom et al., 2005). In principle, a consumption of not more than ca 1% per day of this pool would thus be enough to satisfy the bacterial carbon demand. At the present stage of knowledge of this system, we do, however, not see it as fruitful to add explicit mechanisms for production of bacterial C-substrates to the model.

We have made no attempt to test statistically the goodness of fit of this >35 parameter simulation model. This would be difficult, and to some extent subjective, with a set of data mostly collected during an open-sea experiment where additional noise presumably arises from uneven initial spatial distribution of the added phosphate and different mixing histories for the different water parcels sampled. Our claim that the model reproduces both the magnitude and the pattern if the observations

thus remains subjective and should obviously not be taken as in any way proving the “truth” of the proposed model. The model is probably most useful if regarded a kind of first order approximation to the eastern Mediterranean microbial food web, amenable to experimental challenges different from those reported here, and thus to future improvement.

Acknowledgements

This work was financed by EU through project CYCLOPS EVK3-CT-1999-00009 and the Norwegian Research Council Project 158936.

References

- Andersen, T., 1997. Pelagic Nutrient Cycles. Springer, Berlin.
- Baretta-Bekker, J.G., Baretta, J.W., Ebenhoh, W., 1997. Microbial dynamics in the marine ecosystem model ERSEM II with decoupled carbon assimilation and nutrient uptake. *Journal of Sea Research* 38, 195–211.
- Bonin, D.J., Bonin, M.C., Berman, T., 1989. Mise en evidence experimentale des facteurs nutritifs limitants de la production du micro-nanoplancton et de l’ultraplancton dans une eau cotiere de la Mediterranee orientale (Haifa Israel). *Aquatic Science* 51, 129–159.
- Bronk, D.A., 1999. Rates of NH₄⁺ uptake, intracellular transformation and dissolved organic nitrogen release in two clones of marine *Synechococcus* spp. *Journal of Plankton Research* 21, 1337–1353.
- Christaki, U., Giannakourou, A., Van Wambeke, F., Gregori, G., 2001. Nanoflagellate predation on auto- and heterotrophic picoplankton in the oligotrophic Mediterranean Sea. *Journal of Plankton Research* 23, 1297–1310.
- Christaki, U., Courties, C., Karayanni, H., Giannakourou, A., Maravelias, C., Kormas, K.A., Lebaron, P., 2002. Dynamic characteristics of *Prochlorococcus* and *Synechococcus* consumption by bacterivorous nanoflagellates. *Microbial Ecology* 43, 341–352.
- Coale, K.H., Johnson, K.S., Fitzwater, S.E., Gordon, R.M., Tanner, S., Chavez, F.P., Ferioli, L., Sakamoto, C., Rogers, P., Millero, F., Steinberg, P., Nightingale, P., Cooper, D., Cochlan, W.P., Landry, M.R., Constantinou, J., Rollwagen, G., Trasvina, A., 1996. A massive phytoplankton bloom induced by an ecosystem-scale iron fertilization experiment in the equatorial Pacific Ocean. *Nature* 383, 495–501.
- Cochlan, W.P., Harrison, P.J., 1991. Uptake of nitrate, ammonium, and urea by nitrogen-starved cultures of *Micromonas pusilla* (Prasinophyceae)—transient responses. *Journal of Phycology* 27, 673–679.
- Dolan, J.R., 1999. Diel periodicity in *Synechococcus* populations and grazing by heterotrophic nanoflagellates: analysis of food vacuole contents. *Limnology and Oceanography* 44, 1565–1570.
- Dubinsky, Z., Berman-Frank, I., 2001. Uncoupling primary production from population growth in photosynthesizing organisms in aquatic ecosystems. *Aquatic Science* 63, 4–17.
- Fagerbakke, K.M., Heldal, M., Norland, S., 1996. Content of carbon, nitrogen, oxygen, sulfur and phosphorus in native aquatic and cultured bacteria. *Aquatic Microbial Ecology* 10, 15–27.
- Flaten, G.A.F., Skjoldal, E.F., Krom, M.D., Law, C.S., Mantoura, R.F.C., Pitta, P., Psarra, S., Tanaka, T., Tselepidis, A., Woodward, E.M.S., Zohary, T., Thingstad, T.F., 2005. Studies of the microbial P-cycle during a Lagrangian phosphate-addition experiment in the Eastern Mediterranean. *Deep-Sea Research II*, this issue [doi:10.1016/j.dsr2.2005.08.010].
- Guillou, L., Jacquet, S., Chretiennot-Dinet, M.J., Vaultot, D., 2001. Grazing impact of two small heterotrophic flagellates on *Prochlorococcus* and *Synechococcus*. *Aquatic Microbial Ecology* 26, 201–207.
- Jansson, M., 1993. Uptake, exchange, and excretion of orthophosphate in phosphate-starved *Scenedesmus-quadracauda* and *Pseudomonas* K7. *Limnology and Oceanography* 38, 1162–1178.
- Kress, N., Thingstad, T.F., Herut, B., Zohary, T., Pitta, P., Psarra, S., Polychronaki, T., Spyres, G., Mantoura, R.F.C., Tanaka, T., Rassoulzadegan, F., Groom, S., Krom, M.D., 2005. Effect of P and N addition to oligotrophic Eastern Mediterranean waters influenced by near-shore waters: A microcosm experiment. *Deep-Sea Research II*, this issue [doi:10.1016/j.dsr2.2005.08.013].
- Krom, M.D., Kress, N., Brenner, S., Gordon, L.I., 1991. Phosphorus limitation of primary productivity in the eastern Mediterranean Sea. *Limnology and Oceanography* 36, 424–432.
- Krom, M.D., Brenner, S., Kress, N., Neori, A., Gordon, L.I., 1993. Nutrient distributions during an annual cycle across a warm-core eddy from the E Mediterranean-Sea. *Deep-Sea Research I-Oceanography Research Paper* 40, 805–825.
- Krom, M.D., Woodward, E.M.S., Herut, B., Kress, N., Carbo, P., Mantoura, R.F.C., Spyres, G., Thingstad, T.F., Wassmann, P., Wexels Riser, C., Kitidis, V., Law, C.S., Zodiatis, G., 2005. Nutrient cycling in the south east Levantine basin of the eastern Mediterranean: results from a phosphorus starved system. *Deep-Sea Research II*, this issue [doi:10.1016/j.dsr2.2005.08.009].
- Lee, S., Fuhrman, J.A., 1987. Relationships between biovolume and biomass of naturally derived marine bacterioplankton. *Applied Environment Microbiology* 53, 1298–1303.
- Martinussen, I., Thingstad, T.F., 1987. Utilization of N, P, and organic C by heterotrophic bacteria. II. Comparison of experiments and a mathematical model. *Marine Ecology Progress Series* 37, 285–293.
- Moutin, T., Thingstad, T.F., Van Wambeke, F., Marie, D., Slawyk, G., Raimbault, O., Claustre, H., 2002. Does competition for nanomolar phosphate supply explain the predominance of the cyanobacterium *Synechococcus*? *Limnology and Oceanography* 47, 1562–1567.
- Pasternak, A., Wassmann, P., Wexels Riser, C., 2005. Does mesozooplankton respond to episodic nutrient inputs in the Eastern Mediterranean? *Deep-Sea Research II*, this issue [doi:10.1016/j.dsr2.2005.09.002].
- Pengerud, B., Skjoldal, E.F., Thingstad, T.F., 1987. The reciprocal interaction between degradation of glucose and ecosystem structure—studies in mixed chemostat cultures of marine-bacteria, algae, and bacterivorous nanoflagellates. *Marine Ecology-Progress Series* 35, 111–117.

- Pitta, P., Stambler, N., Tanaka, T., Zohary, T., Tselepidis, A., Rassoulzadegan, F., 2005. Biological response to P addition in the Eastern Mediterranean Sea: The microbial race against time. *Deep-Sea Research II*, this issue [doi:10.1016/j.dsr2.2005.08.012].
- Psarra, S., Zohary, T., Krom, M.D., Mantoura, R.F.C., Polychronaki, T., Stambler, N., Tanaka, T., Tselepidis, A., Thingstad, T.F., 2005. Phytoplankton response to a Lagrangian phosphate addition in the Levantine Sea (Eastern Mediterranean). *Deep-Sea Research II*, this issue [doi:10.1016/j.dsr2.2005.08.015].
- Thingstad, T.F., 1987. Utilization of N, P, and organic C by heterotrophic bacteria .1. outline of a chemostat theory with a consistent concept of maintenance metabolism. *Marine Ecology-Progress Series* 35, 99–109.
- Thingstad, T.F., Pengerud, B., 1985. Fate and effect of allochthonous organic material in aquatic microbial ecosystems. An analysis based on chemostat theory. *Marine Ecology Progress Series* 21, 47–62.
- Thingstad, T.F., Rassoulzadegan, F., 1995. Nutrient limitations, microbial food webs, and biological C-pumps—suggested interactions in a P-limited Mediterranean. *Marine Ecology-Progress Series* 117, 299–306.
- Thingstad, T.F., Havskum, H., Kaas, H., Nielsen, T.G., Riemann, B., Lefevre, D., Williams, P.J.L.B., 1999a. Bacteria-protist interactions and organic matter degradation under P-limited conditions: analysis of an enclosure experiment using a simple model. *Limnology and Oceanography* 44, 62–79.
- Thingstad, T.F., Perez, M., Pelegri, S., Dolan, J., Rassoulzadegan, F., 1999b. Trophic control of bacterial growth in microcosms containing a natural community from northwest Mediterranean surface waters. *Aquatic Microbial Ecology* 18, 145–156.
- Thingstad, T.F., Krom, M.D., Mantoura, R.F.C., Flaten, G.A.F., Groom, S., Herut, B., Kress, N., Law, C.S., Pasternak, A., Pitta, P., Psarra, S., Rassoulzadegan, F., Tanaka, T., Tselepidis, A., Wassmann, P., Woodward, E.M.S., Riser, C.W., Zodiatis, G., Zohary, T., 2005. Nature of phosphorus limitation in the ultraoligotrophic eastern mediterranean. *Science* 309, 1068–1071.
- Turley, C.M., Bianchi, M., Christaki, U., Conan, P., Harris, J.R.W., Psarra, S., Ruddy, G., Stutt, E.D., Tselepidis, A., Van Wambeke, F., 2000. Relationship between primary producers and bacteria in an oligotrophic sea—the Mediterranean and biogeochemical implications. *Marine Ecology-Progress Series* 193, 11–18.
- Vadstein, O., 1997. Evaluation of competitive ability of two heterotrophic planktonic bacteria under phosphorus limitation. *Aquatic Microbial Ecology* 14, 119–127.
- Vadstein, O., Olsen, Y., 1989. Chemical composition and phosphate uptake kinetics of limnetic bacterial communities cultured in chemostats under phosphorus limitation. *Limnology and Oceanography* 34, 939–946.
- Vadstein, O., Jensen, A., Olsen, Y., Reinertsen, H., 1988. Growth and phosphorus status of limnetic phytoplankton and bacteria. *Limnology and Oceanography* 33, 489–503.
- Zohary, T., Robarts, R.D., 1998. Experimental study of microbial P limitation in the eastern Mediterranean. *Limnology and Oceanography* 43, 387–395.
- Zohary, T., Herut, B., Krom, M.D., Mantoura, R.F.C., Pitta, P., Psarra, S., Rassoulzadegan, F., Stambler, N., Tanaka, T., Thingstad, T.F., Woodward, E.M.S., 2005. P-limited bacteria but N and P co-limited phytoplankton in the Eastern Mediterranean—a microcosm experiment. *Deep-Sea Research II*, this issue [doi:10.1016/j.dsr2.2005.08.011].
- Zubkov, M.V., Fuchs, B.M., Tarran, G.A., Burkill, P.H., Amann, R., 2003. High rate of uptake of organic nitrogen compounds by *Prochlorococcus* cyanobacteria as a key to their dominance in oligotrophic oceanic waters. *Applied Environmental Microbiology* 69, 1299–1304.